

Exploring Sparse Visual Prompt for Domain Adaptive Dense Prediction

Senqiao Yang^{1,2*}, Jiarui Wu^{1,3*}, Jiaming Liu^{1*†}, Xiaoqi Li¹, Qizhe Zhang¹,
Mingjie Pan¹, Yulu Gan¹, Zehui Chen⁴, Shanghang Zhang¹ [∞]
¹Peking University, ²Harbin Institute of Technology, Shenzhen,
³Beihang University, ⁴University of Science and Technology of China

Abstract

The visual prompts have provided an efficient manner in addressing visual cross-domain problems. In previous works, (Gan et al. 2022a) first introduces domain prompts to tackle the classification Test-Time Adaptation (TTA) problem by placing image-level prompts on the input and fine-tuning prompts for each target domain. However, since the image-level prompts mask out continuous spatial details in the prompt-allocated region, it will suffer from inaccurate contextual information and limited domain knowledge extraction, particularly when dealing with dense prediction TTA problems. To overcome these challenges, we propose a novel Sparse Visual Domain Prompts (SVDP) approach, which applies minimal trainable parameters (e.g., 0.1%) to pixels across the entire image and reserves more spatial information of the input. To better apply SVDP in extracting domain-specific knowledge, we introduce the Domain Prompt Placement (DPP) method to adaptively allocates trainable parameters of SVDP on the pixels with large distribution shifts. Furthermore, recognizing that each target domain sample exhibits a unique domain shift, we design Domain Prompt Updating (DPU) strategy to optimize prompt parameters differently for each sample, facilitating efficient adaptation to the target domain. Extensive experiments were conducted on widely-used TTA and continual TTA benchmarks, and our proposed method achieves state-of-the-art performance in both semantic segmentation and depth estimation tasks. Project page: Senqiaoyang.com/project/svdp

Introduction

Deep neural networks can achieve promising performance if test data is of the same distribution as the training data. However, it is not the common case in real-world scenarios (Radsoavovic et al. 2022), which contain diverse and disparate domains. When applying a pre-trained model in real-world tasks, the domain gap commonly exists (Sakaridis, Dai, and Van Gool 2021), leading to significant performance degradation on target data. Though we can manually collect labeled data for each real-world target domain, it is laborious and time-consuming (Chen, Wu, and Jiang 2022). To this

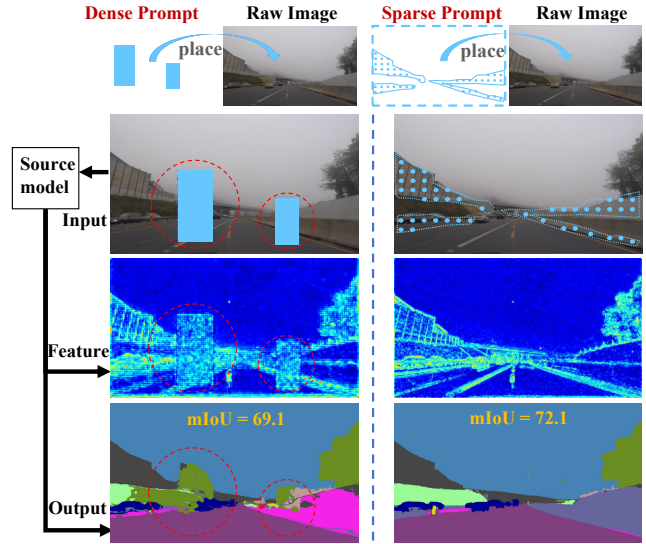


Figure 1: **The motivation and main idea of our method.** (a) Previous dense visual domain prompts (VDP) mask out consecutive spatial details in the placed regions as shown in red circles. In dense prediction DA problems, applying dense VDP will lead to inaccurate context information extraction and severe performance degradation. (b) We introduce Sparse Visual Domain Prompts (SVDP), which are tailored for addressing the occlusion problem of pixel-wise information and can better extract local domain knowledge for cross-domain learning. Though the parameters of SVDP are less than VDP, SVDP achieves better semantic segmentation performance in the Test Time Adaptation.

end, the domain adaptation (DA) methods are introduced and have drawn growing attention in the community.

While DA extensively investigates to address distribution shifts, its typical assumption involves access to raw source data. However, in real-world scenarios, raw data often cannot be publicly accessible due to data protection regulations. Meanwhile, traditional DA methods present resource-intensive backward computation, leading to high training costs (Ganin and Lempitsky 2015). To address this, Test-time adaptation (TTA) (Liang, He, and Tan 2023) is gained significant attention, which tackles distribution shifts at test

*Equal contribution: yangsenqiao.ai@gmail.com,

†Project leader: jiamingliu@stu.pku.edu.cn,

∞ Corresponding author: shanghang@pku.edu.cn

time with only unlabeled test data streams. Prior TTA studies (Wang et al. 2021, 2022a; Chen et al. 2022a; Goyal et al. 2022) predominantly focus on model-based adaptation, utilizing model parameters to fit target domain knowledge.

To better solve the TTA problem, motivated by the recent advances of prompting in NLP (Li and Liang 2021; Liu et al. 2023), VDP (Gan et al. 2022a) first introduces a prompt-based method to tackle the classification TTA problem. It employs image-level prompts to enhance domain transfer efficiency and effectiveness. Specifically, it randomly places the dense prompt on the input image and fine-tunes it to extract target domain knowledge. However, this prompt-based technique encounters limitations when applied to dense prediction tasks such as semantic segmentation and depth estimation TTA. Specifically, the dense prompts obscure continuous spatial information in the allocated regions, as illustrated in Figure 1 (a). This occlusion introduced by prompts leads to incomplete semantic knowledge representation, thereby negatively impacting the quality of segmentation maps. Simultaneously, the occluded details within corresponding features impede the extraction of adequate domain knowledge during cross-domain learning.

To this end, as shown in Fig.1 (b), we propose a novel Sparse Visual Domain Prompts (SVDP) approach for effectively extracting target domain knowledge, specially designed to combat domain shifts in dense prediction tasks. By introducing sparse prompts, which apply minimal trainable parameters (e.g., 0.1%) to pixels across the entire image, more spatial information from the input is preserved. Furthermore, the semantic information can be extracted sufficiently (shown in line 2), leading to noticeable improvements in segmentation outcomes (shown in line 3). In order to better apply SVDP in the pixel-wise TTA task, we propose the Domain Prompt Placement (DPP) to adaptively allocate trainable parameters of SVDP on the pixel with large distribution shifts. In this way, SVDP excels at extracting local domain knowledge, facilitating the transfer of pixel-wise data distribution from the source to the target domain. Furthermore, recognizing that each target domain sample exhibits a unique domain shift, we design a Domain Prompt Updating (DPU) method to optimize prompt parameters efficiently during the TTA process. Specifically, based on the extent of the domain gap observed in target domain samples, we employ varying weights to update the visual prompts. It’s worth noting that we are the pioneers in designing specific strategies for pixel-level placement and image-level optimization in vision prompt learning, which work in synergy to address domain shifts in dense prediction TTA tasks.

Since data privacy and transmission limit access to source data in the real world, we evaluate our method on semantic segmentation and depth estimation source-free adaptation settings, including online TTA (Liang, Hu, and Feng 2020) and Continual Test-Time Adaptation (Wang et al. 2022a) (CTTA). Our proposed approach demonstrates superior performance compared to most state-of-the-art (SOTA) methods across three benchmarks, covering Cityscapes to ACDC (Sakaridis, Dai, and Van Gool 2021) and KITTI (Geiger, Lenz, and Urtasun 2012) to DrivingStereo (Yang et al. 2019). The main contributions are shown as follows:

- 1) We are the first to introduce the visual prompt approach to the dense prediction TTA problem. We propose a novel Sparse Visual Domain Prompts (SVDP) approach to better extract local domain knowledge and transfer pixel-wise data distribution from the source to the target domain.

- 2) In order to efficiently apply SVDP in pixel-wise TTA tasks, we propose the Domain Prompt Placement (DPP) method to adaptively allocate trainable parameters in SVDP based on the degree of distribution shift at the pixel level. And Domain Prompt Updating (DPU) is designed to optimize prompt parameters differently for each sample, facilitating efficient adaptation on target domains.

- 3) We conduct extensive experiments to evaluate the effectiveness of our method, which outperforms most SOTA methods on four TTA and two CTTA benchmarks, covering semantic segmentation and depth estimation tasks.

Related Work

Test-time adaptation

Test-time adaptation (TTA), (Boudiaf et al. 2023; Kundu et al. 2020; Liang, Hu, and Feng 2020; Yang et al. 2021), aims to adapt a source model to an unknown target domain distribution without using any source domain data. Recent research has focused on using self-training or entropy regularization to fine-tune the source model. Specifically, SHOT (Liang, Hu, and Feng 2020) optimizes only the feature extractor using information maximization and pseudo labeling. AdaContrast (Chen et al. 2022b) also uses pseudo labeling for TTA, but introduces self-supervised contrastive learning to enhance performance. In addition to model-level adaptation, (Boudiaf et al. 2022) adjusts the output distribution to address this problem. Tent (Wang et al. 2021) updates the training parameters in the batch normalization layers by entropy minimization. Recent works (Niu et al. 2023; Yuan, Xie, and Li 2023) follow Tent to continually explore the robustness of normalization layers in the TTA process. While the aforementioned works primarily focus on classification tasks, there has been a recent surge of interest in performing TTA on dense prediction tasks (Shin et al. 2022; Song et al. 2022; Zhang et al. 2021).

Continual Test-Time Adaptation (CTTA) is a scenario in which the target domain is not static, increasing challenges for traditional TTA methods (Wang et al. 2022a). (Wang et al. 2022a) serves as the first approach to tackle this task, using a combination of bi-average pseudo labels and stochastic weight reset. While (Wang et al. 2022a; Song et al. 2023) addresses the continual shifts at the model level, (Gan et al. 2022a) leverages visual domain prompts to address the problem in the classification task at the input level for the first time. In this paper, we evaluate our approach on both TTA and CTTA with a specific focus on the dense prediction task.

Prompt learning

Visual prompts are inspired by their counterparts (Liu et al. 2021) which are used in natural language processing (NLP). Language prompts are presented as text instructions to improve the pre-trained language model’s understanding of

downstream tasks (Brown et al. 2020). Recently, researchers have attempted to discard text encoders and use prompts directly for visual tasks. (Bahng et al. 2022) employs visual prompts to pad input images, enabling pre-trained models to adapt to new tasks. Rather than fine-tuning the entire model, VPT (Conder et al. 2022; Jia et al. 2022a; Sandler et al. 2022; Wang et al. 2022b) inserts prompts into image or feature-level patches to adapt Transformer-based models. While these approaches all utilize opaque-block prompts, such prompts can cause performance degradation in dense prediction tasks. **Domain prompts** are first introduced in DAPL (Ge et al. 2022), which proposes a novel prompt learning paradigm for unsupervised domain adaptation (UDA). Embedding domain information using prompts can minimize the cost of fine-tuning and enable efficient domain adaptation. Recognizing the potential of prompt learning for UDA, MPA (Chen, Wu, and Jiang 2022) proposes multi-prompt alignment for multi-source UDA. DePT (Gao et al. 2022a) combines domain prompts with a hierarchical self-supervised regularization for TTA, which aims to solve the error accumulation problem in self-training. (Gan et al. 2022a) further divides domain prompts into domain-specific ones and domain-agnostic ones to address the more challenging CTDA task. However, these studies mainly focus on simple classification DA tasks. Our method, for the first time, applies sparse domain prompts to dense prediction DA tasks. Besides, we are the first to design specific placement and updating strategies for the domain prompt method, which helps to jointly ease the domain shift.

Method

Preliminaries

Test Time Adaptation (TTA) (Liang, He, and Tan 2023) aims at adapting a pre-trained model with parameters trained on the source data ($\mathcal{X}_S, \mathcal{Y}_S$) to multiple unlabeled target data distribution $\mathcal{X}_{T_1}, \mathcal{X}_{T_2}, \dots, \mathcal{X}_{T_n}$ at inference time. The entire process can not access any source domain data and can only access target domain data once. $\mathcal{X}_{T_i} = \{x_i^T\}_{i=1}^{N_t}$, where N_t denotes the scale of the target domain. The upcoming target domain can be a single one (TTA) or multiple continually changing distributions (CTDA), the latter of which is a more realistic setting that requires the model to achieve stability while preserving plasticity.

Domain Prompt. Inspired by language prompt in NLP, (Gan et al. 2022a) first introduces visual domain prompt (VDP) serving as a reminder to continually adapt to the target domain for the classification task, which aims to extract target domain-specific knowledge. Specifically, VDP (\mathbf{p}) are dense learnable parameters added to the input image.

$$\tilde{\mathbf{x}} = \mathbf{x} + \mathbf{p} \quad (1)$$

where \mathbf{x} represents the original input image. The reformulated image $\tilde{\mathbf{x}}$ will serve as the input for our model instead.

Motivation

Sparse Visual Domain Prompt. Traditional visual prompts (Jia et al. 2022b) are deployed on the image or feature level to realize fine-tuning by updating a small number of prompt

parameters. Recent works (Gan et al. 2022a; Gao et al. 2022b) explore visual prompts in classification DA problems, which extract domain knowledge for the target domain and transfer data distribution from the source to the target domain. However, DePT (Gao et al. 2022b) concatenates the domain prompts with class token and image tokens to the input of transformer layers, which neglect the local domain knowledge extraction. Meanwhile, VDP (Gan et al. 2022a) randomly set the locations of dense prompts on the input image, masking out continuous spatial details in prompt allocated regions. Different from classification cross-domain learning, dense prediction DA not only requires global domain knowledge but also relies on extracting intact local domain knowledge. As shown in Fig.1(a), partial spatial information deficiency caused by dense prompts will lead to inaccurate contextual information and negative effects on target domain knowledge extraction. This observation motivates us to propose a novel Sparse Visual Domain Prompts (SVDP), which is tailored for pixel-wise prediction DA tasks. It inserts minimal trainable parameters into pixels across the entire image and reserves more spatial information.

Domain Prompt Placement. Previous work (Gan et al. 2022a; Gao et al. 2022b) randomly put the prompts on the target domain image to extract global domain knowledge. Specifically, it may set prompts on regions with trivial domain shifts, hindering the extraction of local domain knowledge. Especially in the source-free TTA setting, we can only access target domain data once, which makes the efficiency of transfer learning crucial. Therefore, we propose Domain Prompt Placement (DPP) which efficiently extracts more domain-specific knowledge and addresses local domain shift. Specifically, we measure the degree of domain gap by general uncertainty scheme (Gal and Ghahramani 2016; Guan et al. 2021; Roy et al. 2022; Gan et al. 2022b) and tactfully place trainable parameters of SVDP on the pixel with large distribution shifts.

Domain Prompt Updating. The amount of prompt parameters is minimal which brings the challenge of fully learning target domain knowledge during TTA process. Meanwhile, the degree of domain shift is not only various on pixels within the image but also on each target domain test sample. It thus motivates us to update prompt parameters differently for each target sample. Therefore, we design a Domain Prompt Updating (DPU) which efficiently optimizes prompt parameters to fit in target domain distribution. Specifically, we adopt the same uncertainty scheme to measure the degree of domain shift for each target sample. According to the degree, we update prompt parameters for the individual sample with different updating weights.

Sparse visual domain prompt

SVDP maintains the same resolution as the input image ($\mathbf{p} \in \mathbb{R}^{H \times W \times 3}$), it only masks out original information by minimal discrete trainable parameters (e.g. 0.1%) on the pixels with large domain shifts. Compared with the previous dense visual prompt, SVDP preserves more contextual information and possesses the capacity to capture local domain knowledge through pixel-wise prompt parameters. The overall framework of our method is shown in Fig .2, and the

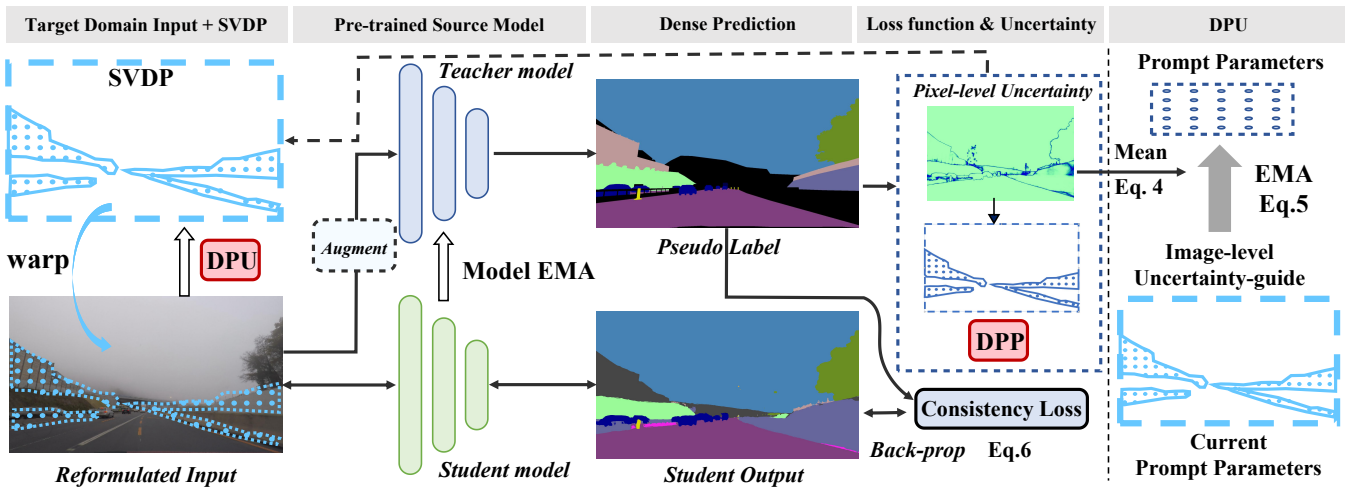


Figure 2: **The overall framework.** **Left:** We warp the SVDP into the image and place prompt parameters on the selected pixel by the Domain Prompt Placement (DPP) method. The reformulated image serves as the input of the teacher and student model. We obtain the uncertainty map as described in Eq. (2) through the teacher model. The uncertainty map is used to evaluate the degree of pixel-level distribution shift. SVDP adopts consistency loss (Eq. (6)) and exponential moving average (EMA) as the optimization strategies. **Right:** Domain Prompt Updating (DPU). Based on the image-level uncertainty value, we adopt different EMA weights to realize stable updating of SVDP parameters, facilitating efficient adaptation to the target domain.

specially designed prompt Placement and Updating methods are introduced in the following.

Domain prompt placing

We propose the Domain Prompt Placement (DPP) strategy of SVDP to efficiently extract local domain knowledge in pixel-wise. We intend to place trainable parameters of SVDP on the pixel with large distribution shifts and adapt pixel-wise data distribution from source to target domain. As shown in Fig. 3, we employ the MC Dropout method (Gal and Ghahramani 2016) to perform m forward propagations ($m = 10$) and obtain m group probabilities for each pixel. Specifically, dropout operation is only applied to the linear layer within the prediction head. Calculating the uncertainty value does not significantly increase the computational cost. Meanwhile, we can also obtain m sets of probabilities through the simpler method of input image resolution augmentation. Inspired by (Roy et al. 2022; Gan et al. 2022b), we calculate the uncertainty value (Eq.(2)) of the input and figure out the pixel-wise degree of domain shift.

$$\mathcal{U}(\tilde{x}_j) = \left(\frac{1}{m} \sum_{i=1}^m \|p_i(\tilde{y}_j|\tilde{x}_j) - \mu\|^2 \right)^{\frac{1}{2}} \quad (2)$$

, where $p_i(\tilde{y}_j|\tilde{x}_j)$ is the predicted probability of input pixel \tilde{x}_j in the i^{th} forward propagation, and μ is the mean prediction (m rounds) of \tilde{x}_j . $\mathcal{U}(\tilde{x}_j)$ thus represents the uncertainty of the source model for pixel-wise target input \tilde{x}_j . As shown in the bottom of Fig. 3, we sort all pixels based on their pixel-wise uncertainty value and place prompt parameters on the pixels with high uncertainty scores.

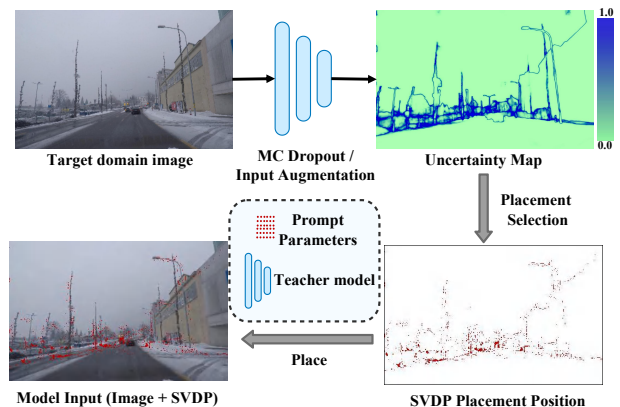


Figure 3: The detailed process of Domain Prompt Placing. The uncertainty map is estimated by MC Dropout (Gal and Ghahramani 2016). The SVDP parameters are placed on the pixels with high uncertainty, then warp into the raw image.

Domain prompt updating

Motivated by the fact that the mean teacher predictions have a higher quality than the standard model (Tarvainen and Valpola 2017a), we utilize a mean-teacher model to provide more accurate predictions in the TTA process. To be specific, we adopt the widely-used exponential moving average (EMA) to achieve the model and prompt updating. Same as previous works (Wang et al. 2022a), the teacher model (\mathcal{T}_{mean}) is updated by EMA from the student model (\mathcal{S}_{target}), shown in Eq. (3):

$$\mathcal{T}_{mean}^t = \alpha \mathcal{T}_{mean}^{t-1} + (1 - \alpha) \mathcal{S}_{target}^t \quad (3)$$

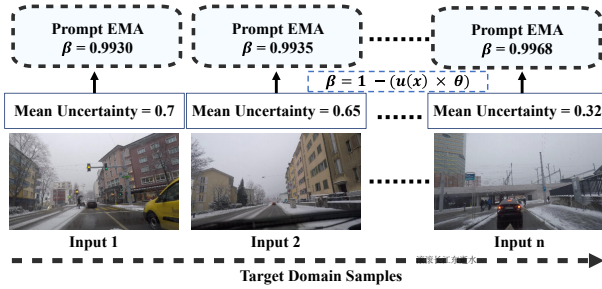


Figure 4: The process of Domain Prompt Updating. We adaptively adjust the prompt EMA updating rate for each target domain sample based on image-level uncertainty value.

When $t = 0$ (t is the time step), we utilize the source domain pre-trained model to initialize the weight of the teacher and student model. And we set $\alpha = 0.999$ (Tavainen and Valpola 2017b), which is the updating weight of EMA.

Different from traditional model updating, we design a special Domain Prompt Updating (DPU) strategy for SVDP to stably fit in target domain distribution. As shown in Fig .4, we adopt image-level uncertainty value to reflect the degree of domain shift for each target domain sample. We calculate the image-level uncertainty value $\mathcal{U}(x)$ by average the pixel-wise uncertainty, shown in Eq. (4):

$$\mathcal{U}(x) = \frac{1}{H \times W} \sum_j^{H \times W} \mathcal{U}(\tilde{x}_j) \quad (4)$$

Based on the image-level uncertainty score, we update prompt parameters for each sample with different weight.

$$p_t = \beta p_{t-1} + (1 - \beta)p_t, \quad (5)$$

Note that, p_t represents the parameters of the SVDP that is updated by Eq. (6). In DPU, we set the prompt EMA updating rate $\beta = 1 - (\mathcal{U}(x) \times \theta)$. θ is intended to bring the value of uncertainty up to the same order of magnitude as the value of the common EMA update parameter (e.g., $\theta = 0.01$). As shown in the top of Fig .4, the prompt EMA weight is set to a large value when the input is of high uncertainty score since the large weight can efficiently adapt to the sample with the large data distribution shift.

Loss function

We utilize teacher model to generate the pseudo labels (\tilde{y}_t), which is refined by test-time augmentation and confidence filter (Wang et al. 2022a). Then, we adopt consistency loss (L_{con}) as the optimization objective for segmentation task, which is a pixel-wise cross-entropy loss (Xie et al. 2021).

$$\mathcal{L}_{con}(\tilde{x}) = -\frac{1}{H \times W} \sum_{w,h}^{W,H} \sum_c^C \tilde{y}_t(w, h, c) \log \hat{y}_t(w, h, c) \quad (6)$$

Where \hat{y}_t is the output of our student model, C means the amount of categories. The loss function of depth estimation is shown in the supplement.

Experiments

In the first subsection, we provide the details of the task settings for test-time adaptation (TTA) and continual TTA (CTTA), as well as a description of the datasets. In the second and third subsections, we compare our method with other baselines (Xie et al. 2021; Wang et al. 2021, 2022a; Gao et al. 2022b,b) in four TTA and two CTTA scenarios. Comprehensive ablation studies are conducted in the last subsection, which investigates the impact of each component. We also provide detailed quantitative analysis and supplementary qualitative analysis in the Appendix.

Task settings and Datasets

TTA and CTTA are commonly used source-free technology in real-world scenarios in which a source pre-trained model adapts to the distribution of an unseen target domain (Liang, He, and Tan 2023). CTTA is of the same setting as TTA but further sets the target domain constantly changing, bringing more difficulties during the continual adaptation process.

Cityscapes-to-ACDC is designed for semantic segmentation cross-domain learning. And we conduct four TTA and one CTTA experiment on the scenario. The source model is an off-the-shelf pre-trained segmentation model that was trained on the Cityscapes dataset (Cordts et al. 2016). The ACDC dataset (Sakaridis, Dai, and Van Gool 2021) contains images collected in four different unseen visual conditions: Fog, Night, Rain, and Snow. For the TTA, we adapt the source pre-trained model to each of the four ACDC target domains separately. For the CTTA, we repeat the same sequence of target domains (Fog→Night→Rain→Snow) multiple times to simulate environment changes in real-world scenarios (Wang et al. 2022a).

KITTI-to-Driving Stereo. To demonstrate the generalization of our method, we also conduct experiments in depth estimation CTTA scenario. The source model employed is an off-the-shelf, pre-trained model, initially trained on the KITTI dataset (Geiger, Lenz, and Urtasun 2012). The Driving Stereo(Yang et al. 2019) comprises images collected under four disparate, unseen visual conditions: foggy, rainy, sunny, and cloudy. For the CTTA, we repeat the same sequence of target domains (Foggy→Rainy→Sunny→Cloudy) multiple times.

Implementation Details. We follow the implementation details (Wang et al. 2022a) to set up our semantic segmentation TTA experiments. Specifically, we use the Segformer-B5 (Xie et al. 2021) pre-trained on Cityscapes as our off-the-shelf source model. We down-sample the original image size of 1920x1080 of the ACDC dataset to 960x540, which serves as network input. We evaluate our predictions under the original resolution. We use a range of image resolution scale factors [0.5, 0.75, 1.0, 1.25, 1.5, 1.75, 2.0] for the augmentation method in the teacher model. For depth estimation CTTA, we follow the implementation details in previous work (Liu et al. 2022) and adopt the pre-trained DPT (Ranftl, Bochkovskiy, and Koltun 2021) on the KITTI as the source model. The optimizer is performed using Adam optimizer (Kingma and Ba 2014) with $(\beta_1, \beta_2) = (0.9, 0.999)$. We set the batch size 1 for both TTA and CTTA experiments

Test-Time Adaptation		Source2Fog		Source2Night		Source2Rain		Source2Snow		Mean-mIoU
Method	REF	mIoU \uparrow	mAcc \uparrow	mIoU \uparrow	mAcc \uparrow	mIoU \uparrow	mAcc \uparrow	mIoU \uparrow	mAcc \uparrow	
Source	NIPS2021 (Xie et al. 2021)	69.1	79.4	40.3	55.6	59.7	74.4	57.8	69.9	56.7
TENT	ICLR2021 (Wang et al. 2021)	69.0	79.5	40.3	55.5	59.9	74.1	57.7	69.7	56.7
CoTTA	CVPR2022(Wang et al. 2022a)	70.9	80.2	41.2	55.5	62.6	75.4	59.8	70.7	58.6
DePT	ICLR2023(Gao et al. 2022b)	71.0	80.2	40.9	55.8	61.3	74.4	59.5	70.0	58.2
VDP	AAAI2023(Gan et al. 2022a)	70.9	80.3	41.2	55.6	62.3	75.5	59.7	70.7	58.5
SVDP	ours	72.1	81.2	42.0	54.9	64.4	76.7	62.2	72.8	60.1\pm0.2

Table 1: **Performance comparison of Cityscapes-to-ACDC TTA.** We use Cityscape as the source domain and ACDC as the four target domains in this setting. Mean-mIoU represents the average mIoU value in four TTA experiments.

Time		$t \longrightarrow$														Mean \uparrow	Gain	
Round		1					2					3						
Method	REF	Fog	Night	Rain	Snow	Mean \uparrow	Fog	Night	Rain	Snow	Mean \uparrow	Fog	Night	Rain	Snow	Mean \uparrow		
Source	NIPS2021 (Xie et al. 2021)	69.1	40.3	59.7	57.8	56.7	69.1	40.3	59.7	57.8	56.7	69.1	40.3	59.7	57.8	56.7	56.7	/
TENT	ICLR2021 (Wang et al. 2021)	69.0	40.2	60.1	57.3	56.7	68.3	39.0	60.1	56.3	55.9	67.5	37.8	59.6	55.0	55.0	55.7	-1.0
CoTTA	CVPR2022(Wang et al. 2022a)	70.9	41.2	62.4	59.7	58.6	70.9	41.1	62.6	59.7	58.6	70.9	41.0	62.7	59.7	58.6	58.6	+1.9
DePT	ICLR2023(Gao et al. 2022b)	71.0	40.8	58.2	56.8	56.5	68.2	40.0	55.4	53.7	54.3	66.4	38.0	47.3	47.2	49.7	53.4	-3.3
VDP	AAAI2023(Gan et al. 2022a)	70.5	41.1	62.1	59.5	58.3	70.4	41.1	62.2	59.4	58.2	70.4	41.0	62.2	59.4	58.2	58.2	+1.5
SVDP	ours	72.1	44.0	65.2	63.0	61.1	72.2	44.5	65.9	63.5	61.5	72.1	44.2	65.6	63.6	61.4	61.1\pm0.3	+4.4\pm0.3

Table 2: **Performance comparison for Cityscape-to-ACDC CTTA.** We take the Cityscape as the source domain and ACDC as the continual target domains. During testing, we sequentially evaluate the four target domains three times. Mean is the average score of mIoU. Gain refers to the improvement achieved by the method compared to the Source model.

and all experiments are conducted on NVIDIA A100 and 3090 GPUs.

The effectiveness on Semantic Segmentation

Cityscapes-to-ACDC TTA. We evaluate the performance of the proposed SVDP on four scenarios with significant domain gap during TTA. Tab .1 shows that the Mean-mIoU for the four domains using the source domain model alone is only 56.7%. Recent advanced methods CoTTA increases it to 58.6% while our method further increases it by 1.5%. These results demonstrate that our method can better address the domain shift problem in test time compared to other methods. Furthermore, in contrast to VDP, which employs dense prompts, our method successfully circumvents the occlusion issue, leading to improved extraction of both semantic and domain knowledge for TTA. In comparison to DePT, which introduces prompts at the token level, our SVDP approach operates at the image-level. This aspect enables the extraction of local domain knowledge, thereby resulting in substantial performance enhancements.

Cityscapes-to-ACDC CTTA. To demonstrate that our method can also address continuously changing domain shifts, we deal with the four domain data during test time periodically. As shown in Tab .2, due to catastrophic forgetting, the performance of TENT and DePT gradually decreases over time. These methods only focus on acquiring new domain-specific knowledge from the target domain, resulting in a neglect of the original knowledge from the source domain. And we find that our method gains 2.5% increase of mIoU more than the previous SOTA CTTA method (Wang et al. 2022a). The results prove that our method can continuously extract target domain knowledge via sparse prompt and preserve previous domain knowledge via model parameters, showing the ability to address dynamic domain shifts. In term of qualitative analysis, shown in Fig .5, our

method correctly distinguishes the sidewalk from the road, avoiding mis-classification in target domains.

Overall, our method outperforms several previous SOTA methods on all semantic segmentation TTA and CTTA tasks and shows promising potential for real-world applications.

The effectiveness on Depth Estimation

KITTI-to-Driving Stereo CTTA. To demonstrate the effectiveness of our approach in addressing CTTA problem in depth estimation task, we conducted a series of evaluations on four distinct target domains from the Driving Stereo dataset at regular intervals during the testing phase. As shown in Table 3, our method consistently outperforms the state-of-the-art (SOTA) technique across all four evaluation metrics. Particularly noteworthy is the significant enhancement in the mean $\delta > 1.25$, achieving a remarkable improvement of 65.9% when compared to the Source model, and an impressive 7.5% improvement over the previous SOTA method. This result underscores the robust continual adaptation ability of our method in the context of depth estimation. Given that CTTA has access to the data only once, as opposed to CoTTA, our approach leverages sparse prompt to effectively adapt to the target domain, resulting in significant performance gains. Overall, these results show that our SVDP consistently attains superior outcomes in the depth estimation tasks.

Ablation study

In this subsection, we evaluate the contribution of each component in our method. Since the CTTA is the most challenging and realistic scenario, we conduct the ablation study on the KITTI-to-Driving Stereo CTTA. **Effectiveness of each component.** As presented in Tab. 4 *Ex2*, Teacher-student (TS) structure is a common technique in CTTA (Wang et al. 2022a; Gan et al. 2022a), which is used to

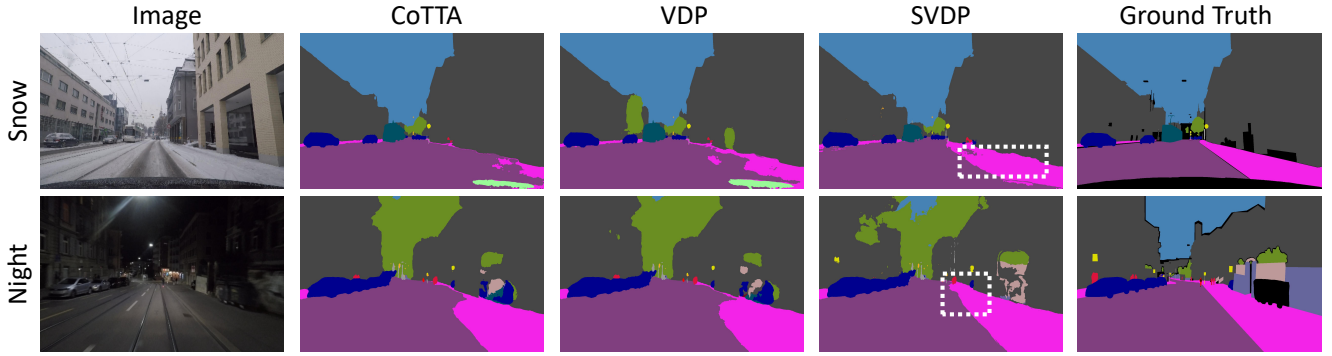


Figure 5: Qualitative comparison of our method with previous SOTA methods on the ACDC dataset. Our method could better segment different pixel-wise classes such as shown in the white box.

Time	$t \rightarrow$																
Domain	Foggy				Rainy				Sunny				Cloudy				Mean \uparrow
Method	$\delta > 1.25\uparrow$	$\delta > 1.25^2\uparrow$	AbsRel \downarrow	RMSE \downarrow	$\delta > 1.25\uparrow$	$\delta > 1.25^2\uparrow$	AbsRel \downarrow	RMSE \downarrow	$\delta > 1.25\uparrow$	$\delta > 1.25^2\uparrow$	AbsRel \downarrow	RMSE \downarrow	$\delta > 1.25\uparrow$	$\delta > 1.25^2\uparrow$	AbsRel \downarrow	RMSE \downarrow	
Source	0.040	0.791	0.313	10.864	0.046	0.573	0.382	15.966	0.153	0.896	0.270	7.404	0.134	0.8697	0.282	7.758	0.093
CoTTA	0.436	0.892	0.268	9.615	0.553	0.791	0.289	12.231	0.597	0.964	0.191	5.445	0.476	0.959	0.203	5.536	0.516
VDP	0.683	0.902	0.159	9.068	0.575	0.692	0.253	15.403	0.716	0.876	0.181	8.905	0.689	0.858	0.197	9.200	0.666
SVDP	0.734	0.943	0.152	7.092	0.689	0.894	0.159	9.700	0.800	0.937	0.168	5.719	0.784	0.930	0.169	5.784	0.741\pm0.03

Table 3: **Performance comparison for KITTI-to-Driving Stereo CTTA.** We take the KITTI as the source domain and Driving Stereo as the continual target domains. Mean is the average score of $\delta > 1.25$ for four domains.

	TS	SVDP	DPP	DPU	Abs Rel \downarrow	$\delta > 1.25\uparrow$
Ex_1					0.312	0.093
Ex_2	✓				0.249	0.503
Ex_3	✓	✓			0.187	0.705
Ex_4	✓	✓	✓		0.169	0.737
Ex_5	✓	✓		✓	0.177	0.723
Ex_6	✓	✓	✓	✓	0.162	0.741

Table 4: **Ablation: Contribution of each component.**

generate pseudo labels in the target domain and only has 0.063 Abs Rel reduces without our method. This verifies the improvement of our method does not come from the usage of this prevalent scheme. In Ex_3 , by introducing sparse prompts (SVDP), we observe that the Abs Rel reduces 0.062 and $\delta > 1.25$ increases 20.2%, respectively. The result demonstrates that SVDP facilitates addressing the domain shift problem, since it can extract local target domain knowledge without damaging the original semantic information. As shown in Ex_4 , DPP achieves further 0.018 Abs Rel reduces and 3.2% $\delta > 1.25$ improvement since the specially designed prompt placement strategy can assist SVDP in extracting target domain-specific knowledge more efficiently. Compared with Ex_3 , DPU (Ex_5) also reduces the Abs Rel 0.01 and improves 1.8% $\delta > 1.25$, respectively. The results prove the effectiveness of DPU and show the importance of adaptively optimizing for different samples during TTA process. Ex_6 shows the complete combination of all components which achieves 64.8% $\delta > 1.25$ improvement and 0.150 Abs Rel reduction in total. It proves that all components compensate each other and jointly address the depth

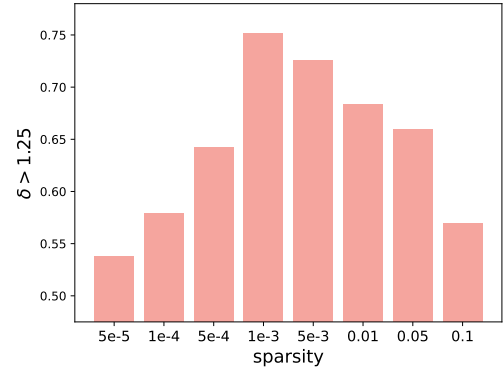


Figure 6: Effect of prompts' sparsity

estimation domain shift problem in test time.

How does the prompt sparsity affect the performance?

As shown in Fig .6, we investigate the performance impact caused by the sparsity of SVDP. Specifically, we gradually increase the density of SVDP pixel-wise parameters and place it into more pixels. We find that $\delta > 1.25$ initially improves along with increasing SVDP density and then starts to decrease when the density exceeds 1e-3. This observation suggests that when SVDP is excessively sparse, it fails to capture the domain-specific knowledge effectively due to the limited number of parameters. In contrast, if the SVDP becomes too dense, the prompt will occlude many spatial details, leading to depth estimation performance degradation. Therefore, it is crucial to strike a balance on the degree of prompt sparsity and we consider that SVDP can achieve optimal potential in 1e-3 sparsity.

Conclusion

In this paper, we are the first to introduce the Sparse Visual Domain Prompt (SVDP) in dense prediction TTA tasks (i.e., semantic segmentation, depth estimation), which address the problem of inaccurate contextual information extraction and insufficient domain-specific feature transferring caused by dense prompt occlusion. Moreover, the Domain Prompt Placement (DPP) and Domain Prompt Updating (DPU) strategies are specially designed for applying SVDP to ease the pixel-wise domain shift better. Our method demonstrates state-of-the-art performance and effectively addresses domain shift through extensive experimentation across various TTA and CTTA scenarios.

Acknowledgments. Shanghang Zhang is supported by the National Key Research and Development Project of China (No.2022ZD0117801). This work was supported by the Emerging Engineering Interdisciplinary Youth Program at Peking University under Grant 7100604372

References

- Bahng, H.; Jahanian, A.; Sankaranarayanan, S.; and Isola, P. 2022. Exploring Visual Prompts for Adapting Large-Scale Models.
- Boudiaf, M.; Denton, T.; van Merriënboer, B.; Dumoulin, V.; and Triantafillou, E. 2023. In Search for a Generalizable Method for Source Free Domain Adaptation.
- Boudiaf, M.; Mueller, R.; Ayed, I. B.; and Bertinetto, L. 2022. Parameter-free Online Test-time Adaptation. *ArXiv*, abs/2201.05718.
- Brown, T. B.; Mann, B.; Ryder, N.; Subbiah, M.; Kaplan, J.; Dhariwal, P.; Neelakantan, A.; Shyam, P.; Sastry, G.; Askell, A.; Agarwal, S.; Herbert-Voss, A.; Krueger, G.; Henighan, T.; Child, R.; Ramesh, A.; Ziegler, D. M.; Wu, J.; Winter, C.; Hesse, C.; Chen, M.; Sigler, E.; Litwin, M.; Gray, S.; Chess, B.; Clark, J.; Berner, C.; McCandlish, S.; Radford, A.; Sutskever, I.; and Amodei, D. 2020. Language Models are Few-Shot Learners.
- Chen, D.; Wang, D.; Darrell, T.; and Ebrahimi, S. 2022a. Contrastive test-time adaptation. In *Proceedings of the IEEE/CVF Conference on Computer Vision and Pattern Recognition*, 295–305.
- Chen, D.; Wang, D.; Darrell, T.; and Ebrahimi, S. 2022b. Contrastive Test-Time Adaptation. *ArXiv*, abs/2204.10377.
- Chen, H.; Wu, Z.; and Jiang, Y.-G. 2022. Multi-Prompt Alignment for Multi-source Unsupervised Domain Adaptation. *arXiv preprint arXiv:2209.15210*.
- Chen, L.-C.; Papandreou, G.; Kokkinos, I.; Murphy, K.; and Yuille, A. L. 2017. Deeplab: Semantic image segmentation with deep convolutional nets, atrous convolution, and fully connected crfs. *IEEE transactions on pattern analysis and machine intelligence*, 40(4): 834–848.
- Conder, J.; Jefferson, J.; Pages, N.; Jawed, K.; Nejadi, A.; and Sagar, M. 2022. Efficient Transfer Learning for Visual Tasks via Continuous Optimization of Prompts.
- Cordts, M.; Omran, M.; Ramos, S.; Rehfeld, T.; Enzweiler, M.; Benenson, R.; Franke, U.; Roth, S.; and Schiele, B. 2016. The cityscapes dataset for semantic urban scene understanding. In *Proceedings of the IEEE conference on computer vision and pattern recognition*, 3213–3223.
- Eigen, D.; Puhrsch, C.; and Fergus, R. 2014. Depth map prediction from a single image using a multi-scale deep network. *Advances in neural information processing systems*, 27.
- Fu, H.; Gong, M.; Wang, C.; Batmanghelich, K.; and Tao, D. 2018. Deep ordinal regression network for monocular depth estimation. In *Proceedings of the IEEE conference on computer vision and pattern recognition*, 2002–2011.
- Gal, Y.; and Ghahramani, Z. 2016. Dropout as a bayesian approximation: Representing model uncertainty in deep learning. In *international conference on machine learning*, 1050–1059. PMLR.
- Gan, Y.; Ma, X.; Lou, Y.; Bai, Y.; Zhang, R.; Shi, N.; and Luo, L. 2022a. Decorate the Newcomers: Visual Domain Prompt for Continual Test Time Adaptation. *arXiv preprint arXiv:2212.04145*.
- Gan, Y.; Pan, M.; Zhang, R.; Ling, Z.; Zhao, L.; Liu, J.; and Zhang, S. 2022b. Cloud-Device Collaborative Adaptation to Continual Changing Environments in the Real-world. *arXiv preprint arXiv:2212.00972*.
- Ganin, Y.; and Lempitsky, V. 2015. Unsupervised domain adaptation by backpropagation. In *International conference on machine learning*, 1180–1189. PMLR.
- Gao, Y.; Shi, X.; Zhu, Y.; Wang, H.; Tang, Z.; Zhou, X.; Li, M.; and Metaxas, D. N. 2022a. Visual Prompt Tuning for Test-time Domain Adaptation.
- Gao, Y.; Shi, X.; Zhu, Y.; Wang, H.; Tang, Z.; Zhou, X.; Li, M.; and Metaxas, D. N. 2022b. Visual Prompt Tuning for Test-time Domain Adaptation. *arXiv preprint arXiv:2210.04831*.
- Ge, C.; Huang, R.; Xie, M.; Lai, Z.; Song, S.; Li, S.; and Huang, G. 2022. Domain Adaptation via Prompt Learning. *ArXiv*, abs/2202.06687.
- Geiger, A.; Lenz, P.; and Urtasun, R. 2012. Are we ready for autonomous driving? the kitti vision benchmark suite. In *2012 IEEE conference on computer vision and pattern recognition*, 3354–3361. IEEE.
- Goyal, S.; Sun, M.; Raghunathan, A.; and Kolter, J. Z. 2022. Test time adaptation via conjugate pseudo-labels. *Advances in Neural Information Processing Systems*, 35: 6204–6218.
- Guan, D.; Huang, J.; Xiao, A.; Lu, S.; and Cao, Y. 2021. Uncertainty-aware unsupervised domain adaptation in object detection. *IEEE Transactions on Multimedia*, 24: 2502–2514.
- Hoyer, L.; Dai, D.; and Van Gool, L. 2022. Daformer: Improving network architectures and training strategies for domain-adaptive semantic segmentation. In *Proceedings of the IEEE/CVF Conference on Computer Vision and Pattern Recognition*, 9924–9935.
- Jia, M.; Tang, L.; Chen, B.-C.; Cardie, C.; Belongie, S.; Har-iharan, B.; and Lim, S.-N. 2022a. Visual Prompt Tuning.
- Jia, M.; Tang, L.; Chen, B.-C.; Cardie, C.; Belongie, S.; Har-iharan, B.; and Lim, S.-N. 2022b. Visual prompt tuning.

- In *Computer Vision—ECCV 2022: 17th European Conference, Tel Aviv, Israel, October 23–27, 2022, Proceedings, Part XXXIII*, 709–727. Springer.
- Kingma, D. P.; and Ba, J. 2014. Adam: A method for stochastic optimization. *arXiv preprint arXiv:1412.6980*.
- Kundu, J. N.; Uppala, P. K.; Pahuja, A.; and Babu, R. V. 2018. Adadepth: Unsupervised content congruent adaptation for depth estimation. In *Proceedings of the IEEE conference on computer vision and pattern recognition*, 2656–2665.
- Kundu, J. N.; Venkat, N.; M, R.; and Babu, R. V. 2020. Universal Source-Free Domain Adaptation.
- Lee, J.-H.; and Kim, C.-S. 2019. Monocular depth estimation using relative depth maps. In *Proceedings of the IEEE/CVF Conference on Computer Vision and Pattern Recognition*, 9729–9738.
- Li, X. L.; and Liang, P. 2021. Prefix-tuning: Optimizing continuous prompts for generation. *arXiv preprint arXiv:2101.00190*.
- Li, Z.; Shi, S.; Schiele, B.; and Dai, D. 2023. Test-time Domain Adaptation for Monocular Depth Estimation. In *2023 IEEE International Conference on Robotics and Automation (ICRA)*, 4873–4879. IEEE.
- Liang, J.; He, R.; and Tan, T. 2023. A comprehensive survey on test-time adaptation under distribution shifts. *arXiv preprint arXiv:2303.15361*.
- Liang, J.; Hu, D.; and Feng, J. 2020. Do We Really Need to Access the Source Data? Source Hypothesis Transfer for Unsupervised Domain Adaptation. In *ICML*.
- Lin, G.; Milan, A.; Shen, C.; and Reid, I. 2017. Refinenet: Multi-path refinement networks for high-resolution semantic segmentation. In *Proceedings of the IEEE conference on computer vision and pattern recognition*, 1925–1934.
- Liu, J.; Zhang, Q.; Li, J.; Lu, M.; Huang, T.; and Zhang, S. 2022. Unsupervised Spike Depth Estimation via Cross-modality Cross-domain Knowledge Transfer. *arXiv preprint arXiv:2208.12527*.
- Liu, P.; Yuan, W.; Fu, J.; Jiang, Z.; Hayashi, H.; and Neubig, G. 2021. Pre-train, Prompt, and Predict: A Systematic Survey of Prompting Methods in Natural Language Processing. *arXiv: Computation and Language*.
- Liu, P.; Yuan, W.; Fu, J.; Jiang, Z.; Hayashi, H.; and Neubig, G. 2023. Pre-train, prompt, and predict: A systematic survey of prompting methods in natural language processing. *ACM Computing Surveys*, 55(9): 1–35.
- Nathan Silberman, P. K., Derek Hoiem; and Fergus, R. 2012. Indoor Segmentation and Support Inference from RGBD Images. In *ECCV*.
- Niu, S.; Wu, J.; Zhang, Y.; Wen, Z.; Chen, Y.; Zhao, P.; and Tan, M. 2023. Towards stable test-time adaptation in dynamic wild world. *arXiv preprint arXiv:2302.12400*.
- Radosavovic, I.; Xiao, T.; James, S.; Abbeel, P.; Malik, J.; and Darrell, T. 2022. Real-World Robot Learning with Masked Visual Pre-training. *CoRL*.
- Ramamonjisoa, M.; Du, Y.; and Lepetit, V. 2020. Predicting Sharp and Accurate Occlusion Boundaries in Monocular Depth Estimation Using Displacement Fields. In *Proceedings of the IEEE/CVF Conference on Computer Vision and Pattern Recognition (CVPR)*.
- Ramamonjisoa, M.; and Lepetit, V. 2019. SharpNet: Fast and Accurate Recovery of Occluding Contours in Monocular Depth Estimation. In *Proceedings of the IEEE/CVF International Conference on Computer Vision (ICCV) Workshops*.
- Ranftl, R.; Bochkovskiy, A.; and Koltun, V. 2021. Vision Transformers for Dense Prediction. *ArXiv preprint*.
- Roy, S.; Trapp, M.; Pilzer, A.; Kannala, J.; Sebe, N.; Ricci, E.; and Solin, A. 2022. Uncertainty-guided source-free domain adaptation. In *Computer Vision—ECCV 2022: 17th European Conference, Tel Aviv, Israel, October 23–27, 2022, Proceedings, Part XXV*, 537–555. Springer.
- Sakaridis, C.; Dai, D.; and Van Gool, L. 2021. ACDC: The adverse conditions dataset with correspondences for semantic driving scene understanding. In *Proceedings of the IEEE/CVF International Conference on Computer Vision*, 10765–10775.
- Sandler, M.; Zhmoginov, A.; Vladymyrov, M.; and Jackson, A. 2022. Fine-tuning Image Transformers using Learnable Memory.
- Scharstein, D.; Hirschmüller, H.; Kitajima, Y.; Krathwohl, G.; Nešić, N.; Wang, X.; and Westling, P. 2014. High-resolution stereo datasets with subpixel-accurate ground truth. In *Pattern Recognition: 36th German Conference, GCPR 2014, Münster, Germany, September 2-5, 2014, Proceedings 36*, 31–42. Springer.
- Shin, I.; Tsai, Y.-H.; Zhuang, B.; Schuster, S.; Liu, B.; Garg, S.; Kweon, I. S.; and Yoon, K.-J. 2022. MM-TTA: Multi-Modal Test-Time Adaptation for 3D Semantic Segmentation.
- Song, J.; Lee, J.; Kweon, I. S.; and Choi, S. 2023. EcoTTA: Memory-Efficient Continual Test-time Adaptation via Self-distilled Regularization. In *Proceedings of the IEEE/CVF Conference on Computer Vision and Pattern Recognition*, 11920–11929.
- Song, J.; Park, K.; Shin, I.; Woo, S.; and Kweon, I. S. 2022. CD-TTA: Compound Domain Test-time Adaptation for Semantic Segmentation.
- Tarvainen, A.; and Valpola, H. 2017a. Mean teachers are better role models: Weight-averaged consistency targets improve semi-supervised deep learning results. *Advances in neural information processing systems*, 30.
- Tarvainen, A.; and Valpola, H. 2017b. Mean teachers are better role models: Weight-averaged consistency targets improve semi-supervised deep learning results. *Learning*.
- Tranheden, W.; Olsson, V.; Pinto, J.; and Svensson, L. 2021. Dacs: Domain adaptation via cross-domain mixed sampling. In *Proceedings of the IEEE/CVF Winter Conference on Applications of Computer Vision*, 1379–1389.
- Wang, D.; Shelhamer, E.; Liu, S.; Olshausen, B. A.; and Darrell, T. 2021. Tent: Fully Test-Time Adaptation by Entropy Minimization. In *ICLR*.

Wang, Q.; Fink, O.; Gool, L. V.; and Dai, D. 2022a. Continual Test-Time Domain Adaptation. *ArXiv*, abs/2203.13591.

Wang, Z.; Zhang, Z.; Lee, C.-Y.; Zhang, H.; Sun, R.; Ren, X.; Su, G.; Perot, V.; Dy, J.; and Pfister, T. 2022b. Learning to Prompt for Continual Learning. In *CVPR*.

Wu, X.; Wu, Z.; Guo, H.; Ju, L.; and Wang, S. 2021. Danet: A one-stage domain adaptation network for unsupervised nighttime semantic segmentation. In *Proceedings of the IEEE/CVF Conference on Computer Vision and Pattern Recognition*, 15769–15778.

Xie, E.; Wang, W.; Yu, Z.; Anandkumar, A.; Alvarez, J. M.; and Luo, P. 2021. SegFormer: Simple and efficient design for semantic segmentation with transformers. *Advances in Neural Information Processing Systems*, 34: 12077–12090.

Xu, D.; Wang, W.; Tang, H.; Liu, H.; Sebe, N.; and Ricci, E. 2018. Structured Attention Guided Convolutional Neural Fields for Monocular Depth Estimation. In *Proceedings of the IEEE Conference on Computer Vision and Pattern Recognition (CVPR)*.

Yang, G.; Song, X.; Huang, C.; Deng, Z.; Shi, J.; and Zhou, B. 2019. DrivingStereo: A Large-Scale Dataset for Stereo Matching in Autonomous Driving Scenarios. In *IEEE Conference on Computer Vision and Pattern Recognition (CVPR)*.

Yang, S.; Wang, Y.; van de Weijer, J.; Herranz, L.; and Jui, S. 2021. Generalized Source-Free Domain Adaptation. *international conference on computer vision*.

Yang, Y.; and Soatto, S. 2020. Fda: Fourier domain adaptation for semantic segmentation. In *Proceedings of the IEEE/CVF Conference on Computer Vision and Pattern Recognition*, 4085–4095.

Yuan, L.; Xie, B.; and Li, S. 2023. Robust test-time adaptation in dynamic scenarios. In *Proceedings of the IEEE/CVF Conference on Computer Vision and Pattern Recognition*, 15922–15932.

Zhang, Y.; Borse, S.; Cai, H.; and Porikli, F. 2021. Aux-Adapt: Stable and Efficient Test-Time Adaptation for Temporally Consistent Video Semantic Segmentation.

Zhao, H.; Shi, J.; Qi, X.; Wang, X.; and Jia, J. 2017. Pyramid scene parsing network. In *Proceedings of the IEEE conference on computer vision and pattern recognition*, 2881–2890.

Zhao, S.; Fu, H.; Gong, M.; and Tao, D. 2019. Geometry-aware symmetric domain adaptation for monocular depth estimation. In *Proceedings of the IEEE/CVF Conference on Computer Vision and Pattern Recognition*, 9788–9798.

Zheng, C.; Cham, T.-J.; and Cai, J. 2018. T2net: Synthetic-to-realistic translation for solving single-image depth estimation tasks. In *Proceedings of the European conference on computer vision (ECCV)*, 767–783.

Appendix Overview

The following items are included in this supplementary material.

- Additional Ablation Studies of
 - Depth Estimation on TTA scenario
 - Domain Prompt Updating
- Qualitative Analysis of
 - Semantic Segmentation
 - Depth Estimation
- Additional Quantitative Results
- Additional Related Work

Additional Ablation Studies

Depth Estimation on TTA scenario

The proposed method comprises a Sparse Visual Prompt (SVDP), a Domain Prompt Placement (DPP) strategy, and a Domain Prompt Updating (DPU) strategy to mitigate domain shifts in semantic segmentation tasks. In this study, we conduct ablation experiments on the TTA scenario (KITTI-to-DrivingStereo Foggy) to evaluate the effectiveness of each component.

To compare the performance of our method with and without using the teacher-student (TS) structure, a common technique in TTA used to generate pseudo labels in the target domain, we present the results in Tab. 5 Ex_2 . The results show that without our method, TS only has 0.069 Abs Rel reduces, indicating that our method’s improvement does not come from the usage of this prevalent scheme. In Ex_3 , we introduce SVDP to extract local target domain knowledge without damaging the original spatial information. The results demonstrate that SVDP achieves a 21.0% $\delta > 1.25$ improvement and 0.073 Abs Rel reduction, effectively addressing the domain shift problem. In Ex_4 , DPP achieves a further 3.3% $\delta > 1.25$ improvement and 0.014 Abs Rel reduces by serving as a specially designed prompt placement strategy to assist SVDP in extracting more target domain-specific knowledge. We evaluate the effectiveness of the DPU in Ex_5 , which adaptively optimizes for different samples during testing. Compared with Ex_3 , DPU reduces the Abs Rel 0.006 and improves 2.2% $\delta > 1.25$ respectively. Finally, in Ex_6 , we show the complete combination of all components, which achieves a total of 69.4% $\delta > 1.25$ improvement and 0.161 Abs Rel reduction. These results demonstrate that all components of our method effectively address the depth estimation domain shift and compensate for each other to achieve superior performance.

Domain Prompt Updating

For SVDP, we utilize Eq.5 to update the prompt parameters and conduct an analysis of the sensitivity of the parameter β in the depth estimation CTTA scenario. As depicted in Fig. 8, we investigate the impact of $\delta > 1.25$ values on the performance. Specifically, we gradually increase the value of β and record the corresponding $\delta > 1.25$ values. We observe that the $\delta > 1.25$ improves with increasing β ; however, it starts to decrease once β exceeds 0.999. Compare

Table 5: Ablation: Contribution of each component on KITTI-to-DrivingStereo Foggy.

	TS	SVDP	DPP	DPU	Abs Rel↓	$\delta > 1.25 \uparrow$
Ex_1					0.313	0.040
Ex_2	✓				0.244	0.482
Ex_3	✓	✓			0.171	0.692
Ex_4	✓	✓	✓		0.157	0.725
Ex_5	✓	✓		✓	0.165	0.714
Ex_6	✓	✓	✓	✓	0.152	0.734

with the best fixed β value, our proposed DPU (red line) strategy can further achieve 1.5% $\delta > 1.25$ improvement. Therefore, due to the different degrees of domain shift, we need to update prompt parameters for the each sample with different EMA weights.

Qualitative analysis

Semantic Segmentation

To further demonstrate the effectiveness of our proposed method, SVDP, we conduct a qualitative comparison with two current leading methods, CoTTA (Wang et al. 2022a) and VDP (Gan et al. 2022a), on the CTTA scenario (Cityscapes-to-ACDC).

The results of the comparison are presented in Fig .7. In the foggy target-domain, we highlight a white box that contains a tall truck object. This object is difficult to segment as it shares characteristics with the *sign* class. Thanks to the contribution of the Domain Prompt Placement (DPP), our proposed method, SVDP, has a significant advantage in dealing with such confusing semantic segmentation categories with high uncertainty. Our method also outperforms CoTTA and VDP in the remaining three domains. In these domains, our proposed method correctly distinguishes the sidewalk from the road, avoiding misclassification. Overall, our method can achieve better local segmentation results and neglect the influence of local domain shift. And our method produces finer results than the previous state-of-the-art methods, with clear visual improvement.

Depth estimation

To demonstrate the generalizability of our proposed method SVDP, we compare it with the current SOTA method on the Depth Estimation task, and the results of the qualitative analysis are shown in Fig. 9

Compared with the VDP and CoTTA, We notice that our SVDP can obviously improve the semantic representation of the model, which concentrates more on the foreground object. The results verify that our methods can extract the target domain knowledge during the test time adaptation. Furthermore, our SVDP enhances the model’s depth estimation ability in the regions of edges, sharpness, and long distances.

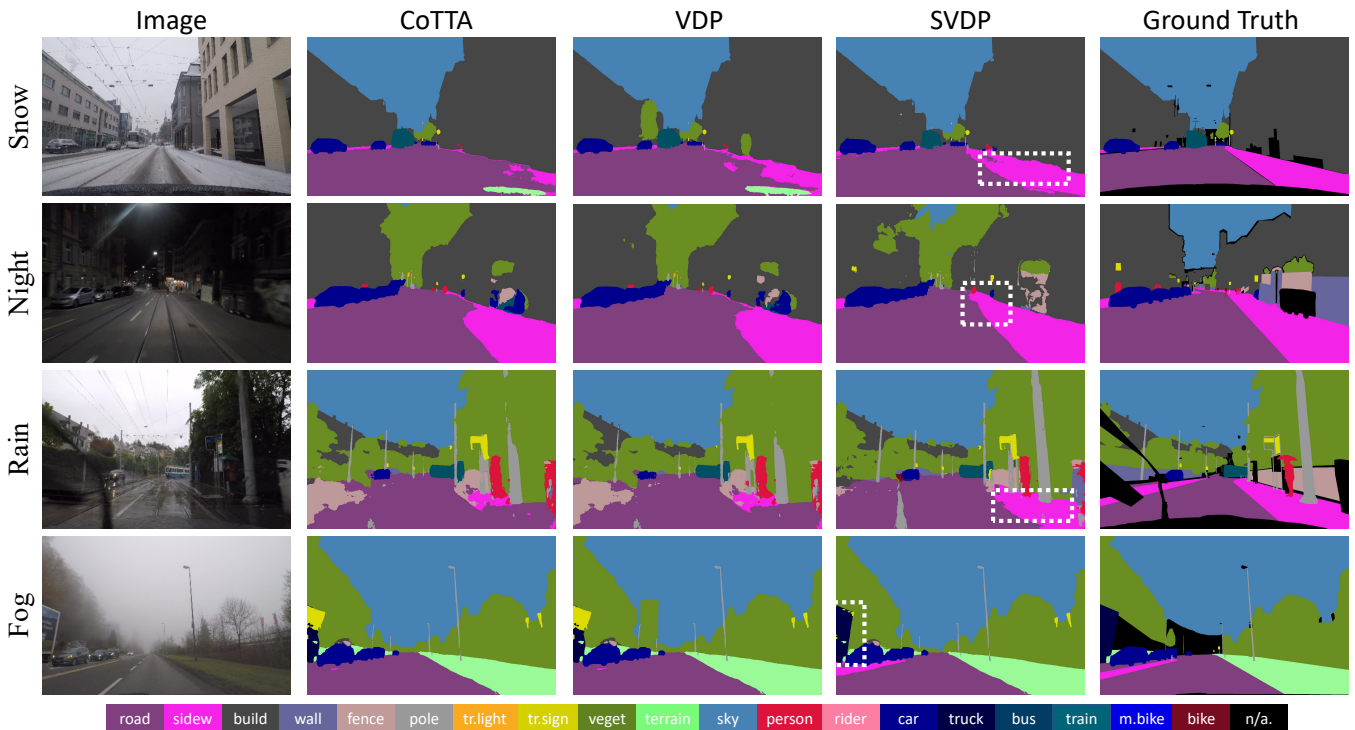


Figure 7: Qualitative comparison of SVDP with previous SOTA method: CoTTA (Wang et al. 2022a), VDP (Gan et al. 2022a) on ACDC Fog, Night, Rain, and Snow four scenarios. SVDP could better segment different pixel-wise classes such as shown in the white box.

Table 6: Performance Comparison for **Cityscapes-to-ACDC Fog domain in TTA scenario**. The IoU score of each class and the mIoU score are reported. The best results are highlighted in **bold**.

Method	road	side.	buil.	wall	fence	pole	light	sign	veg.	terr.	sky	pers.	rider	car	truck	bus	train	mbike	bike	mIoU
Source	94.0	63.9	79.8	55.7	24.9	45.0	41.5	69.8	86.6	71.0	97.6	64.1	66.2	87.4	73.0	92.6	87.7	50.2	61.7	69.1
TENT	94.0	64.0	79.7	55.4	24.6	44.6	41.4	69.9	86.7	71.1	97.6	64.0	65.9	87.4	73.0	92.6	88.0	50.2	61.9	69.0
CoTTA	93.9	63.6	80.0	55.5	25.1	49.0	43.4	73.0	87.0	70.7	97.8	68.6	71.3	87.1	74.8	93.6	89.1	58.0	66.7	70.9
DePT	94.0	64.0	79.9	56.1	25.3	48.8	43.5	73.0	87.1	70.6	97.5	67.9	71.5	87.3	75.1	93.5	89.1	57.4	66.5	71.0
VDP	93.9	63.6	80.0	55.6	25.1	49.0	43.4	73.0	86.9	70.7	97.7	68.5	71.1	87.2	74.7	93.5	89.2	57.9	66.6	70.9
SVDP	94.4	65.9	80.5	57.8	26.5	50.5	43.9	73.6	87.6	72.0	98.0	68.8	71.3	87.7	77.6	94.4	92.6	60.0	67.4	72.1

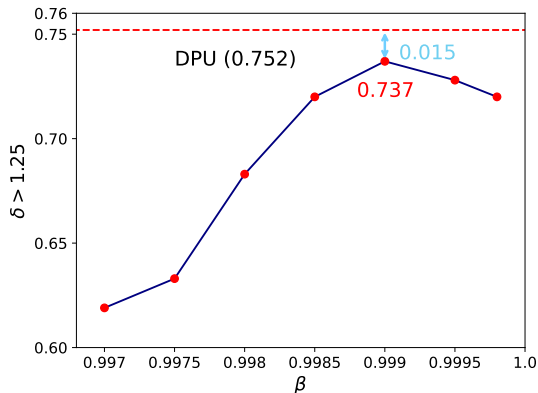


Figure 8: Sensitivity Analysis: The effect of prompt EMA's parameter β on depth estimation performance in the CTTA scenario.

Additional Quantitative Results

We present a comprehensive presentation of experimental results on the Test-time adaptation task for Cityscapes-to-ACDC, as shown in Tab . 6 - Tab . 9. Our findings suggest that our proposed approach can better address the domain shift problem and achieve better IoU value in most categories.

Additional related work

Semantic segmentation is a crucial task in many computer vision applications aimed at assigning a categorical label to every pixel in an image. Several representative works in this field include DeepLab (Chen et al. 2017), PSPNet (Zhao et al. 2017), RefineNet (Lin et al. 2017), and Segformer (Xie et al. 2021). Despite their high performance, these methods usually require extensive amounts of pixel-level annotated data, which can be laborious and time-consuming to collect. Additionally, they may suffer from poor generalization

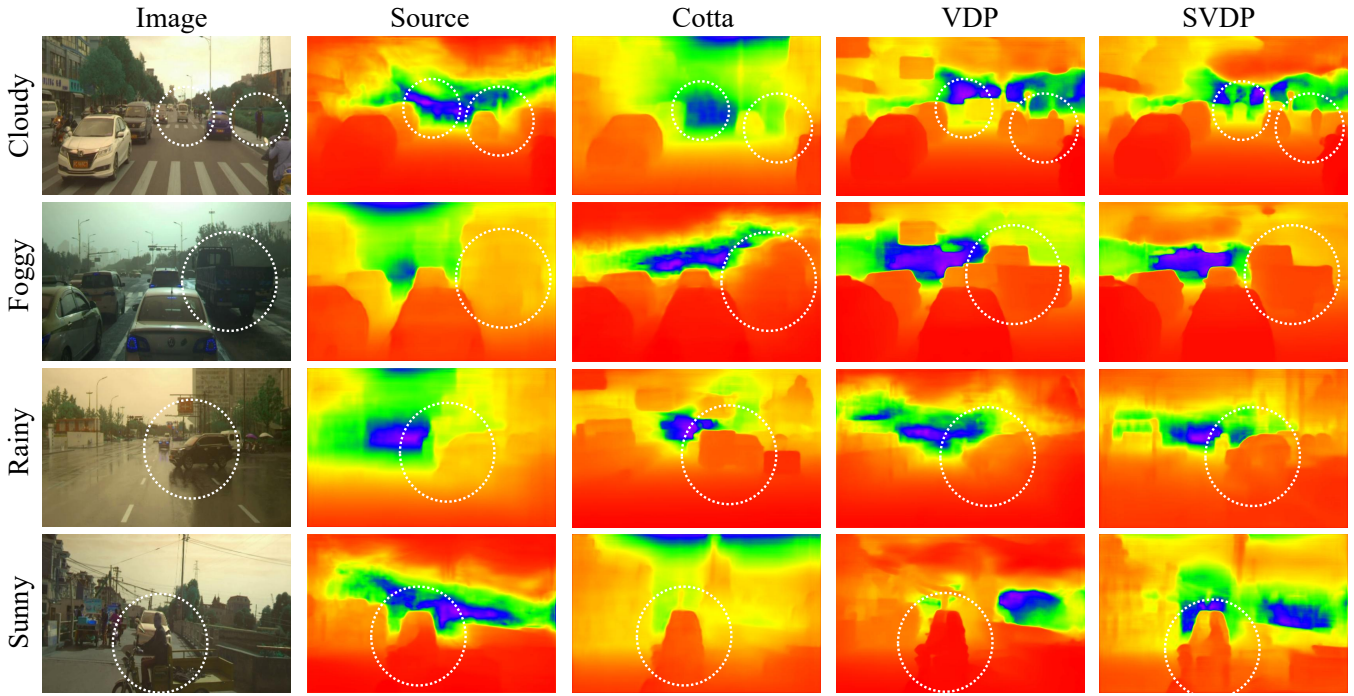


Figure 9: Qualitative comparison of SVDP with previous SOTA method: CoTTA(Wang et al. 2022a), VDP(Gan et al. 2022a) on Driving Stereo Cloudy, Foggy, Rainy, and Sunny four scenarios. SVDP could make the depth estimation better such as shown in the white circle.

Table 7: Performance Comparison for **Cityscapes-to-ACDC Night domain in TTA scenario**. The IoU score of each class and the mIoU score are reported. The best results are highlighted in **bold**.

Method	road	side.	buil.	wall	fence	pole	light	sign	veg.	terr.	sky	pers.	rider	car	truck	bus	train	mbike	bike	mIoU
Source	87.6	46.3	61.8	27.0	25.3	40.8	38.7	39.4	47.7	26.8	11.4	48.6	39.9	76.1	15.9	24.2	52.0	26.5	29.6	40.3
TENT	87.7	46.4	61.9	27.1	25.2	40.8	38.8	39.3	47.0	26.8	9.6	48.7	40.0	76.2	16.1	24.3	51.9	26.6	29.7	40.2
CoTTA	87.6	46.7	62.3	27.2	25.0	44.0	42.9	40.8	47.2	26.7	8.8	51.8	41.9	76.6	18.8	22.4	51.7	27.8	32.1	41.2
DePT	87.3	46.5	62.0	27.0	25.3	43.5	40.9	41.0	47.2	26.6	8.8	51.0	42.5	77.1	17.5	23.0	51.5	26.4	31.7	40.9
VDP	87.6	46.8	62.2	27.1	25.0	44.0	42.9	41.0	47.3	26.6	9.0	51.7	41.9	76.6	18.7	23.2	51.9	27.8	32.0	41.2
SVDP	87.5	46.6	52.7	28.3	23.1	46.0	44.7	41.2	56.1	23.9	10.5	53.4	43.2	78.0	25.7	26.0	46.9	29.7	34.1	42.0

Table 8: Performance Comparison for **Cityscapes-to-ACDC Rain domain in TTA scenario**. The IoU score of each class and the mIoU score are reported. The best results are highlighted in **bold**.

Method	road	side.	buil.	wall	fence	pole	light	sign	veg.	terr.	sky	pers.	rider	car	truck	bus	train	mbike	bike	mIoU
Source	82.3	47.1	89.5	36.8	26.6	51.0	64.8	62.9	89.5	60.3	97.8	46.0	53.0	81.1	25.3	65.4	56.7	47.6	51.2	59.7
TENT	82.4	46.7	89.6	37.3	27.0	50.6	64.6	62.9	89.5	60.4	97.7	46.7	54.5	81.2	25.4	65.2	56.6	47.3	51.8	59.9
CoTTA	83.0	48.4	90.2	38.3	28.0	55.5	68.1	67.5	90.3	61.2	98.0	54.1	60.1	82.0	27.4	67.0	59.1	50.9	55.4	62.6
DePT	82.0	47.3	89.8	37.5	26.9	53.0	66.2	65.8	89.6	60.8	97.7	52.8	59.5	81.6	26.5	66.5	57.9	49.5	53.2	61.3
VDP	83.0	48.3	90.2	38.2	28.0	55.5	68.2	67.5	90.2	61.2	97.9	54.1	59.9	82.0	27.5	67.0	59.1	50.9	55.3	62.3
SVDP	85.2	54.4	91.1	43.1	31.8	57.7	69.2	69.9	90.8	62.1	98.2	56.5	60.7	83.0	28.7	67.6	63.6	55.0	55.7	64.4

Table 9: Performance Comparison for **Cityscapes-to-ACDC Snow domain in TTA scenario**. The IoU score of each class and the mIoU score are reported. The best results are highlighted in **bold**.

Method	road	side.	buil.	wall	fence	pole	light	sign	veg.	terr.	sky	pers.	rider	car	truck	bus	train	mbike	bike	mIoU
Source	79.8	40.8	86.9	43.6	46.5	56.4	72.3	65.5	82.9	5.7	97.1	62.8	40.4	85.4	54.7	44.5	73.1	22.7	36.0	57.8
TENT	79.6	40.0	86.8	43.4	46.5	56.1	72.2	65.6	82.9	5.7	97.1	63.0	40.9	85.5	54.7	43.1	72.7	23.0	36.5	57.7
CoTTA	80.1	40.7	87.5	43.9	47.7	59.9	75.3	69.2	84.0	5.1	97.2	67.3	46.9	86.2	56.1	43.4	74.1	25.7	43.3	59.8
DePT	79.1	40.6	86.8	43.4	47.5	59.8	75.1	69.4	83.5	5.2	97.1	67.2	46.5	86.3	56.0	44.0	73.9	25.6	43.1	59.5
VDP	80.1	40.8	87.5	43.9	47.8	59.9	75.1	69.4	83.9	5.1	97.2	67.2	46.7	86.2	56.2	43.9	74.0	25.7	42.9	59.7
SVDP	86.6	57.7	88.2	47.0	45.5	62.4	75.9	71.5	84.9	3.9	97.4	68.0	49.3	87.1	57.1	49.2	77.5	26.8	45.4	62.2

when applied to new domains. Recent research has focused on addressing these challenges through domain adaptation strategies. For instance, (Yang and Soatto 2020) proposes a method that swaps the low-frequency spectrum to align the source and target domains. (Tranheden et al. 2021) mixes the images from both domains, along with their corresponding labels and pseudo-labels. In contrast, (Wu et al. 2021) uses adversarial learning to train a domain adaptation network for nighttime semantic segmentation. (Hoyer, Dai, and Van Gool 2022) develops a novel model and training strategies to enhance training stability and avoid overfitting to the source domain. However, these methods often require re-training the model on the source domain, which is inconvenient. Furthermore, they need to be retrained when adapting to a new target domain, incurring additional time and resource costs. Therefore, we propose SVDP to efficiently address the domain shift problem, which leverages a pre-trained model on the source domain and adds only a few parameters to achieve strong generalization capabilities on the target domain.

Depth estimation Depth estimation is a crucial task of machine scene comprehension. The ascendancy of deep learning has established it as the dominant approach for supervised depth estimation across both outdoor (Eigen, Puhrsch, and Fergus 2014; Geiger, Lenz, and Urtasun 2012; Yang et al. 2019) and indoor settings (Nathan Silberman and Fergus 2012; Scharstein et al. 2014). Typical methodologies involve the integration of a universal encoder, responsible for assimilating global context, alongside a decoder designed to retrieve depth details (Xu et al. 2018; Ramamonjisoa, Du, and Lepetit 2020; Lee and Kim 2019; Ramamonjisoa and Lepetit 2019; Fu et al. 2018). In the context of cross-domain depth estimation, the emphasis is on aligning source and target domains either at the input or feature level (Kundu et al. 2018; Zheng, Cham, and Cai 2018; Zhao et al. 2019). As a case in point, the work presented in (Zhao et al. 2019) introduced a geometry-centric symmetric adaptation framework, conceived to optimize both the translation and the depth estimation processes simultaneously. (Li et al. 2023) combines the self-supervised model and the supervised model to tackle this problem. However, these methods always lead to catastrophic forgetting, and thus we introduce the Sparse Visual Domain Prompt to tackle this problem.